DOI https: //doi. org/10.1007/s11595-022-2566-3

Substrate Effect on the Structural and Electrical Properties of $LaNiO_3$ Thin Films

YAO Dan[1*], WANG Weiwei[2], YU Jiangying[1], YOU Yuwei[1]

(1.Key Laboratory of Advanced Electronic Materials and Devices, School of Mathematics & Physics, Anhui Jianzhu University, Hefei 230601, China; 2.Department of Materials, Hefei Guoxuan High-Tech Power Energy Co., Ltd, Hefei 230011, China)

Abstract: Epitaxial $LaNiO_3$ (LNO) thin films prepared from the sols modified with polyethyleneimine (PEI) were grown on single-crystal $LaAlO_3$, $(LaAlO_3)_{0.3}(SrAlTaO_6)_{0.7}$, and $SrTiO_3$ substrates, respectively, using a simple polymer assisted deposition (PAD). The epitaxial structure, surface morphologies and transport of the LNO films were studied by X-ray diffraction ($\theta/2\theta$ symmetric scan, ω-scan, and in-plane φ-scan), the field emission scanning electron microscopy, and a standard dc four-probe method. It is found that, compared with that of LNO bulk, the c-axis parameter of the LNO film increases under compressive strain and decreases under tensile strain. All the LNO films exhibit metal properties in the temperature-dependent resistivity. The resistivity of the LNO films shows an increasing trend with the lattice mismatch strain changing from compressive to tensile. It is suggested that the oxygen vacancy compensated by more Ni^{2+} changed from Ni^{3+} in the film increases with the strain changing from compressive to tensile, which results in the increase of the resistivity.

Key words: nickelates; electrical properties; epitaxial film; polymer assisted deposition

1 Introduction

Epitaxial thin-film technology has the potential to change the functionality of conventional crystals in a way to achieve better performance and novel properties. Thin films of perovskite oxides with low electrical resistivity, such as $La_{0.5}Sr_{0.5}CoO_3$[1], $SrRuO_3$[2], and $LaNiO_3$ (LNO)[3], have been receiving considerable attention because of the fact that such a physical property makes them suitable electrodes for perovskite ferroelectric layers in thin film capacitors. Among them, LNO due to its high stability and conductivity has been widely investigated, which is rhombohedral with the room temperature lattice constant of c=0.546 nm, a=0.384 nm[4]. It has a good match with most of perovskite-type ferroelectric materials including PZT and BST. Moreover, LNO displays low resistivity and good metallic conductivity in a wide range of temperature, roughly from 1 to 1 000 K[5]. Therefore, the LNO film is a promising candidate of an electrode for perovskite-type ferroelectric materials.

Generally, the synthesis of bulk $LaNiO_3$ materials needs extreme conditions of high temperature and high oxygen pressure to stabilize Ni^{3+} oxidation state since the Ni^{3+} state is thermodynamically unstable. Researchers turn to the preparation of the LNO films to facilitate the experimental study and application because the synthesis of bulk LNO compound is very difficult. Over the past few years, many efforts have been paid to prepare the LNO thin films by different methods including pulsed laser deposition (PLD), molecular beam epitaxy[6], chemical solution deposition (CSD)[7], radio-frequency magnetron sputtering (RF)[8], metal organic decomposition (MOD)[9], and so on. Most of all these vacuum techniques require high-cost equipment and strict deposition condition and those derived films can not be fabricated on a large scale. Although chemical methods are more cost-effective, they are not considered competitive in producing high quality films required for fundamental studies and highly demanding applications since the deposited films crack easily during heat treatment.

Recently polymer assisted deposition (PAD) has been demonstrated as a novel technique to grow both simple and complex metal oxide thin films[10,11]. In this process, the mixture of metal precursor and soluble polymer is used to form a solution with desired viscosity without gelling. The polymer not only actively binds the metal ions but also encapsulates the metal

(Received: May 17, 2021; Accepted: Nov. 10, 2021)

*Corresponding author: YAO Dan(姚丹): Lecturer; Ph D; E-mail: yaodan1212@ahjzu.edu.cn

Funded by the Natural Science Foundation of Anhui Jianzhu University(No. 2019QDZ63)

ions to prevent premature precipitation and formation of metal oxide oligomers. The PAD method has been successfully applied in the growth of simple and complex metal oxide films. In this paper, we successfully fabricate the LNO thin films using PAD, and investigate the substrate effects on the structure and properties of the resulting LNO films. The results demonstrated that oxygen deficiency was spontaneously generated in strained LNO thin films, and has finely influenced on the electrical properties of them. The results also provide insights into the effect of oxygen deficiency on the correlated phase in rare-earth nickelates.

2 Experimental

LNO thin films were prepared by a polymer assisted deposition method. $La(NO_3)_3 \cdot 5H_2O$,$Ni(NO_3)_3 \cdot 6H_2O$ were converted into metal nitrates by dissolving in distilled water to get the transparent precursor solution with the cationic stoichiometry ratio La:Ni=1:1. Appropriate amount of ethylenediaminetetra acetic acid (EDTA) and polyethyleneimine (PEI) were added into the solution, and then the above solution was subjected to continuous stirring for several hours at 60 ℃ to get proper viscosity. The solution was deposited on 0.5 cm×0.5 cm (001) $LaAlO_3$ (LAO), (001) $(LaAlO_3)_{0.3}(SrAlTaO_6)_{0.7}$(LSAT), and (001)$SrTiO_3$ (STO) single crystal substrates by spin coatingwith the rotation speed of 5000 r/min for 30 s. Finally, all deposited thin films were annealed in a tube furnace at 750 ℃ for 2 h under air atmosphere. X-ray diffraction (XRD) patterns were recorded on a Panalytical X' pert, X-ray diffractometer with Cu Kα (λ=1.540 6 Å) at room temperature. The Field emission scanning electron microscopy (FE-SEM, JSM-6700F) was employed to observe the surface morphology and the thickness. X-ray photoelectron spectroscopy (XPS) analyses were performed using an ESCALAB 250 system (Thermal Scientific). The temperature dependence of resistivity was carried by the standard four-probe standard dc four-probe method using silver coatings between 80 K and 300 K.

3 Results and discussion

3.1 Thickness and morphological characterization of the LNO films

Fig.1(a) shows cross-sectional scanning electron microscopy images of LNO films grown by PAD method on these substrates. As shown in the picture, the thicknesses of the LNO films on different substrates are similar and about 70 nm. From Figs.1(d)-1(f), it can be found that the surface of films show some noticeable microcracks and a few voids distribution, which are common characteristics of films by chemical solution deposition and could be attributed to the gradual removing of EDTA and PEI by calcinations in the process of sample preparation.

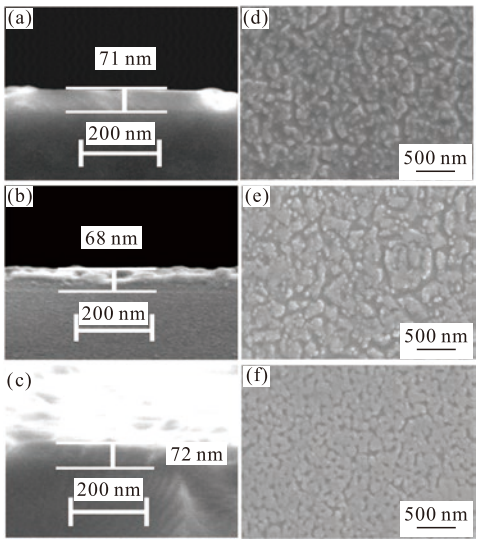

Fig.1 SEM images of the corresponding cross-sectional areas and surface of LNO films on LAO (Figs.1a, 1d); LSAT (Figs.1b, 1e); STO (Figs.1c, 1f) substrates, respectively

Fig.2 shows the standard θ-2θ XRD patterns for LNO thin films grown on (001) LAO, LSAT, and STO substrates, respectively. Only LNO reflection peaks (pseudocubic notation) close to the reflection of substrates were found, suggesting that all the LNO films are single phase with a similar orientation to the substrates. Insets of Fig.2 show the rocking curves (ω-scan) of LNO peaks and the values of full-width-half-maximum (FWHM) are listed in the Table 1, the relatively small values indicate good crystalline quality of these films. The in-plane crystal plane alignment between the film and the substrate was determined by the typical φ-scan. As shown in Fig.3, in-plane φ-scans of (110) LNO and (110) substrates are nearly identical with four peaks separated by 90°, indicating filmswere in-plane aligned as well. The heteroepitaxial relationship between the LNO film and the (001)-oriented substrates can be described as (001) LNO// (001) LAO, (001) LSAT, and (001) STO, consistent with films deposited by other techniques. The above descriptions demonstrate that high-purity and good epitaxial growths of LNO films have been successfully obtained on these substrates by using this convenient PAD method. It is widely known that the bulk LNO has a rhombohedral perovskite structure with a lattice parameter of 3.838

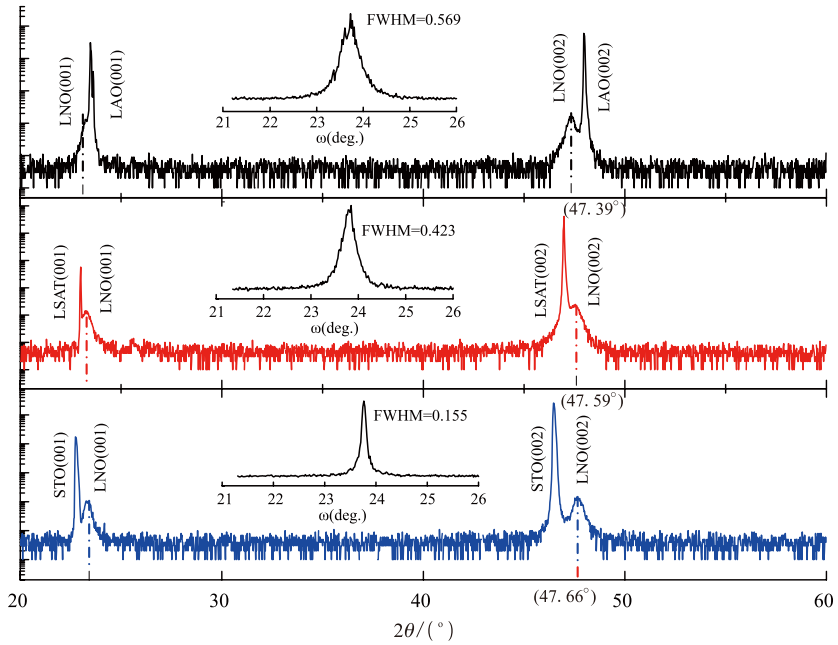

Fig.2 XRD patterns of θ-2θ scans for the $LaNiO_3$ films grown on LAO, LSAT, and STO substrates. Insets are the plots of (002) ω-scan (rocking-curve) for each film

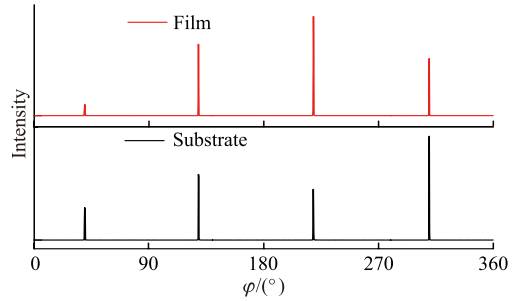

Fig.3 XRD patterns of φ scans for (110) plane reflection of LNO film on LAO, LSAT, and STO substrates

Table 1 Lattice mismatch, FWHM of the rocking curves for (002) peaks, c-axis lattice parameter, Ni^{3+}/Ni^{2+} ratio and value of δ (oxygen vacancy) of LNO films on LAO, LSAT, and STO substrates, respectively

Substrate	FWHM/(°)	Lattice mismatch	c/(Å)	Ni^{3+}/Ni^{2+}	δ
LAO	0.569	−1.3%	3.834	3.545	0.11
LSAT	0.423	0.6%	3.818	2.571	0.14
STO	0.155	1.7%	3.813	2.195	0.16

Å, corresponding to a compressive strain of −1.3% on LAO (a_{LAO} = 3.79 Å), and tensile strains of 0.6% on LSAT (a_{LSAT} = 3.86 Å) and 1.7% on STO (a_{STO} = 3.905 Å). Therefore, the strain result an elongation along the out-of-plane axis on LAO, while a reduction in the out-of-plane axis on LSAT and STO, which was indeed observed in the high-resolution XRD θ-2θ scans and the out-of-plane lattice parameters (Table 1) were calculated from the positions of film reflections using Bragg formula.

3.2 Electrical properties of the films

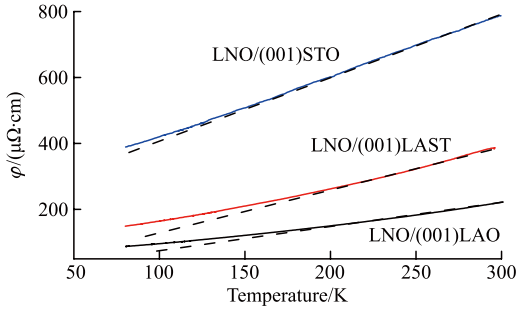

Fig.4 Resistivity versus temperature plots of LNO thin films on LAO, LSAT, and STO substrates, 80 K<T< 300 K. The dotted lines are guides to the eye

Fig.4 shows the resistivity versus temperature characteristics of LNO films on LAO, LSAT, and STO substrates, respectively, measured by a standard four-probe technique with silver contacts. It is observed that resistivity of the films decreases monotonically with the decrease of temperature, characteristic of a metallic behavior. Furthermore, a careful inspection of $\rho(T)$ curves of all films indicates that there are at least two different behaviors of in the temperature range investigated: (a) at temperatures above 150 K, where $\rho(T)$ is linear; and (b) at temperatures below 150 K, where $\rho(T)$ is larger than expected for a linear behavior (in Fig.4). These behaviors are quite similar to reported those of bulk samples and films prepared in other methods[12,13,14]. The resistivity of the LNO films on LAO, LSAT, and STO are 222, 383, and 787 μΩ·cm at room tempera-

ture, respectively. This is consistent with the reported values derived from PLD method (340 μΩ·cm) [8] and much smaller than that of polycrystalline thin film on Si (111) substrate. The temperature coefficient [1/ρdρ/dT] of LNO// (001) LAO resistivity was calculated to be about $2.48\times10^{-3}\,K^{-1}$ in the region with temperatures greater than 200 K, which was also the same as the value $2.48\times10^{-3}\,K^{-1}$ reported in the Refs.[12,14]. These results are further evidence that polymer assisted deposition is a successful method to grow epitaxial LNO films

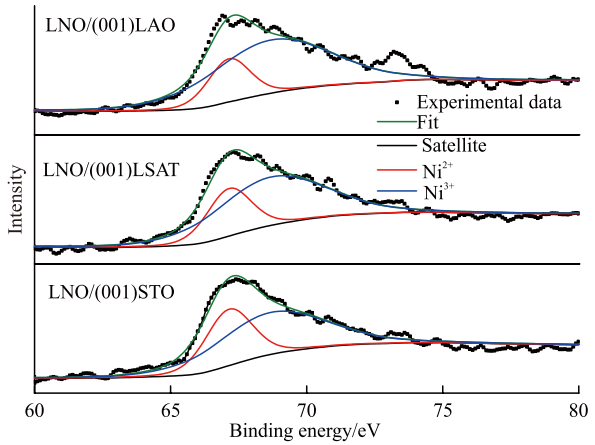

Fig.5 The typical XPS spectra of LNO films on LAO, LSAT, and STO substrates related to Ni (3p) core level

To obtain further insight into the electronic structures of LNO films on different substrates, XPS measurements were carried out, as shown in Fig.5. Due to the coupling of spin-orbit splitting and multiple splitting, it is challenging to obtain the best fit of the as-measured XPS signals at the Ni 2p edge due to the strong La 3d core-level background[14,15]. XPS spectra at the Ni 3p edge were used to extract the binding energies of divalent Ni^{2+} and trivalent Ni^{3+} states. To ensure the quality of the peak fitting, a Shirley background and a combined Lorentzian-Gaussian method is applied. The fitting results for all films are presented in Fig.5. The peak at 66.9 eV (A) and 68.9 eV can be assigned to Ni^{2+} $3p_{3/2}$ and Ni^{3+} $3p_{3/2}$ which is consistent with the reported results[16]. By calculating the area of the fitted curves, we extracted the portions of Ni^{3+} and Ni^{2+} oxidation states in the three films. Based on these results, the Ni^{3+}/ Ni^{2+} ratios can thus be calculated, which are shown in Table 1. As a result, the exact chemical formula for $LaNiO_{3-\delta}$// (001) LAO, (001) LSAT, and (001) STO should be $LaNiO_{2.89}$(δ=0.11), $LaNiO_{2.86}$(δ=0.14), and $LaNiO_{2.81}$(δ=0.16), respectively. The oxygen vacancy shows an increasing trend with the lattice mismatch strain changing from compressive to tensile. Similar results are also reported for the oxygen vacancy of $NdNiO_3$ films[17] and other perovskite oxides[18,19]. For stoichiometric LNO, the metal property mainly comes from overlap between the conduction band of Ni 3d and fulfilled valence band of O 2p[20]. The content of Ni^{2+} with bigger radius increased as the decrease of Ni^{3+}/Ni^{2+} ratio, which leads to the stretched length of Ni-O bond. It has been generally accepted that overlap between the valence band and conduction band would decrease with the stretched length of Ni-O bond, bringing with higher value of electrical resistivity. Previous study has shown that when Ni^{3+}/Ni^{2+} is equal to 1, that is, the system of $LaNiO_{2.75}$ would to be a semiconductor[21].

4 Conclusions

In summary, we were successfully fabricated epitaxial $LaNiO_3$ thin films on single-crystal (001) LAO, LSAT, and STO substrates in terms of PAD technique the unique using of soluble polymer and processing design of PAD provide stable and homogeneous solutions at a molecular level that allows the epitaxial growth of high-quality thin films. The resistivity of the LNO films shows increasing trend with the strain changing from compressive to tensile, which results from the increase of the oxygen vacancies compensated by more Ni^{2+} changed from Ni^{3+} in the film.

References

[1] Song JM, Luo LH, Dai XH, *et al.* Switching Properties of Epitaxial $La_{0.5}Sr_{0.5}CoO_3/Na_{0.5}Bi_{0.5}TiO_3/La_{0.5}Sr_{0.5}CoO_3$ Ferroelectric Capacitor[J]. *RSC Advances*, 2018, 8 (8): 4 372-4 376

[2] Noguchi Y, Maki H, Kitanaka Y, *et al.* Control of Misfit Strain in Ferroelectric $BaTiO_3$ Thin-film Capacitors With $SrRuO_3$-based Electrodes on (Ba, Sr)TiO_3-buffered $SrTiO_3$ Substrates[J]. *Applied Physics Letters*, 2018, 113 (1): 129 031-129 035

[3] Matavz A, Kovac J, Cekada M, *et al.* Enhanced Electrical Response in Ferroelectric Thin Film Capacitors with Inkjet-printed $LaNiO_3$ Electrodes[J]. *Applied Physics Letters*, 2018,113 (1): 129 041-129 044

[4] Rajeev KP, Shivashankar GV, Raychaudhuri AK. Low-temperature Electronic Properties of a Normal Conducting Perovskite Oxide ($LaNiO_3$)[J]. *Solid State Communications*, 1991, 79 (7): 591-595

[5] Wu D, Li AD, Liu ZG, *et al.* Fabrication And Electrical Properties Of Sol-Gel Derived (BaSr)TiO_3 Thin Films with Metallic $LaNiO_3$ Elec trode[J]. *Thin Solid Film*s, 1998, (336): 172-175

[6] Wrobel F, Mark AF, Christiani G, *et al.* Comparative Study of $LaNiO_3$/$LaAlO_3$ Heterostructures Grown by Pulsed Laser Deposition And Oxide Molecular Beam Epitaxy[J]. *Applied Physics Letters*, 2017, 110(4):

416 061-416 065

[7] Duan ZF, Cui Y, Yang Z, *et al.* Growth of Highly c-axis Oriented $LaNiO_3$ Films with Improved Surface Morphology on Si Substrate Using Chemical Solution Deposition and Rapid Heat Treatment Process[J]. *Ceramics International*, 2018, 44 (1): 695-702

[8] Wakiya N, Azuma T, Shinozaki K, *et al.* Low-temperature Epitaxial Growth of Conductive $LaNiO_3$ Thin Films by RF Magnetron Sputtering[J]. *Thin Solid Films*, 2002, 410 (1): 114-120

[9] Li AD, Ge CZ, Lu P, *et al.* Preparation of Perovskite Conductive $LaNiO_3$ Films by Metalorganic Decomposition[J]. *Applied Physics Letters* 1996, 68 (10): 1 347-1 349

[10] Zou GF, Zhao J, Luo HM, *et al.* Polymer-Assisted-Deposition: A Chemical Solution Route for a Wide Range of Materials[J]. *Chemical Society Reviews*, 2013, 42 (2): 439-449

[11] Vila Fungueirino JM, Rivas Murias B, Juan Rubio Zuazo, *et al.* Polymer Assisted Deposition of Epitaxial Oxide Thin Films[J]. *Journal of Materials Chemistry C*, 2018, 6 (15): 3 834-3 844

[12] Mambrini GP, Leite ER. Structural Microstructural, and Transport Properties of Highly Oriented $LaNiO_3$ Thin Films Deposited on $SrTiO_3$ (100) Single Crystal[J]. *Journal of Applied Physics*, 2007, 102(4): 437 081-437 084

[13] Escote MT, Pontes FM, Leite ER, *et al.* Microstructural and Transport Properties of $LaNiO_3$ Films Grown on Si (111) by Chemical Solution Deposition[J]. *Thin Solid Films*, 2003, 445(1): 54-58

[14] Jin San Choi, Chang Won Ahn, Jong-Seong Bae, *et al.* Identifying a Perovskite Phase in Rare-Earth Nickelates Using X-ray Photoelectron Spectroscopy[J].*Current Applied Physics*, 2020, 20 (1): 102-105

[15] Jin San Choi, Muhammad Sheeraz, Jong-Seong Bae, *et al.* Effect of Ceramic-target Crystallinity on Metal-to-insulator Transition of Epitaxial Rare-earth Nickelate Films Grown by Pulsed Laser Deposition[J]. *ACS Applied Electronic Materials*, 2019, 1 (9): 1 952-1 958

[16] QIAO L, Bi XF. Direct Observation of Ni^{3+} And Ni^{2+} in Correlated $LaNiO_3$ Films[J]. *EPL*, 2011, 93: 570 021-570 026

[17] Feungyang Heo, Chadol Oh, Junwoo Son, *et al.* Influence of Tensile-Strain-Induced Oxygen Deficiency on Metal-Insulator Transitions in $NdNiO_{3-\delta}$ Epitaxial Thin Films[J]. *Scientific Reports*, 2017, 7: 46 811-46 819

[18] Aschauer U, Pfenninger R, Selbach SM, *et al.* Strain-Controlled Oxygen Vacancy Formation and Ordering in $CaMnO_3$[J]. *Physical Review B*, 2013, (5)88: 054111 1-054111 7

[19] Akihiro Kushima, Sidney Yip, Bilge Yildiz. Competing Strain Effects in Reactivity of $LaCoO_3$ With Oxygen[J]. *Physical Review B* , 2010,(11)82:115435 1-115435 6

[20] Torrance JB, Lacorre P, Nazzal AI, *et al.* Systematic Study of Insulator-Metal Transitionsin Perovskites $RniO_3$(R=Pr, Nd, Sm, Eu) due to Closing of Charge-Transfer Gap[J]. *Physical Review B* , 1992, 45 (14): 8 209-8 212

[21] Sanchez RD, Causa MT, Caneiro A, *et al*. Metal-Insulator Transition in Oxygen-Deficient $LaNiO_{3-X}$ Perovskites[J]. *Physical Review* B, 1996, 54(23): 16 574-16 578